INTERNATIONAL JOURNAL OF SYSTEMS SCIENCE
2024, VOL. 55, NO. 7, 1283–1303
https://doi.org/10.1080/00207721.2024.2304665

Taylor & Francis
Taylor & Francis Group

Safe-by-construction autonomous vehicle overtaking using control barrier functions and model predictive control

Dingran Yuan[a], Xinyi Yu[b], Shaoyuan Li[a] and Xiang Yin[a]

[a]Department of Automation, Shanghai Jiao Tong University, Shanghai, People's Republic of China; [b]Department of Computer Science, University of Southern California, Los Angeles, CA, USA

ABSTRACT

Ensuring safety for vehicle overtaking systems is one of the most fundamental and challenging tasks in autonomous driving. This task is particularly intricate when the vehicle must not only overtake its front vehicle safely but also consider the presence of potential opposing vehicles in the opposite lane that it will temporarily occupy. In order to tackle the overtaking task in such challenging scenarios, we introduce a novel integrated framework tailored for vehicle overtaking manoeuvres. Our approach integrates the theories of varying-level control barrier functions (CBF) and time-optimal model predictive control (MPC). The main feature of our proposed overtaking strategy is that it is safe-by-construction, which enables rigorous mathematical proof and validation of the safety guarantees. We show that the proposed framework is applicable when the opposing vehicle is either fully autonomous or driven by human drivers. To demonstrate our framework, we perform a set of simulations for overtaking scenarios under different settings. The simulation results show the superiority of our framework in the sense that it ensures collision-free and achieves better safety performance compared with the standard MPC-based approach without safety guarantees.

ARTICLE HISTORY
Received 16 October 2023
Accepted 7 January 2024

KEYWORDS
Overtaking manoeuvres; formal methods; control barrier functions; autonomous driving

1. Introduction

1.1. Motivation

Over the past decade, smart vehicle control systems have garnered significant attention due to advancements in real-time computing and advanced control theory. The benefits of implementing smart controls have been widely acknowledged, including improved traffic arrangements, reduced accidents and enhanced driving comfort (Meng et al., 2018; Xu et al., 2022; Zhou et al., 2022). In particular, high-level intelligent vehicle control can be broadly categorised into four main groups: adaptive cruise control (ACC), lane keeping (LK), lane change (LC) and *overtaking*. Among these categories, overtaking manoeuvres present a distinctive challenge due to their requirement to consider the interaction with other vehicles in the adjacent lane. One of the most formidable challenges in above vehicle control tasks arises in the context of two-way road overtaking scenarios, as depicted in Figure 1. Here, the vehicle faces the dual responsibility of safely overtaking its front vehicle while also preventing possible collision with the potential opposing vehicles in the opposite lane that it will temporarily occupy. A study by the German Insurers Accident Research (UDV) revealed that the accident rate, measured in accidents per 10^6 vehicles km, during overtaking on a two-way road is approximately 50% higher than that on a one-way lane without opposing traffic (Richter et al., 2017). This stark statistic underscores not only the importance but also the complexity associated with addressing this two-way road overtaking problem, which motivates the study in this paper.

As autonomous vehicles become increasingly human-centered and safety-critical, there is an increasing demand for *formal safety guarantees* in the analysis and design of autonomous driving strategies. The recent advancement in control barrier functions, such as those proposed by Ames et al. (2017, 2019), Xiao and Belta (2022), offer a crucial avenue. These advanced tools provide a systematic approach to ensuring safety, particularly relevant in the safety assurance of autonomous overtaking systems as they have a much lower computational

CONTACT Shaoyuan Li syli@sjtu.edu.cn Department of Automation, Shanghai Jiao Tong University, Shanghai200240, People's Republic of China

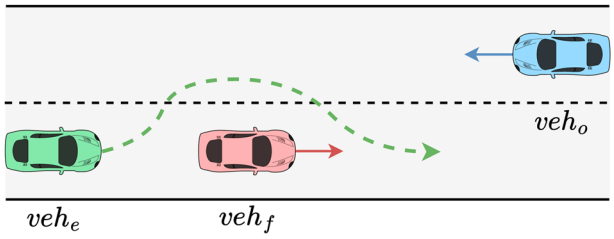

Figure 1. A two-way road overtaking scenario with possible opposing traffic.

complexity compared with reachability-based methods (Herbert et al., 2021). Existing studies often rely on model-based methods (Chae & Yi, 2020; Hu et al., 2021; Usman & Kunwar, 2009) or data-driven methods (Hu et al., 2014; Li, Qiu et al., 2020; Milanés et al., 2012) for vehicle overtaking manoeuvres design, but their inability to offer rigorous safety guarantees in dynamic environments underscores the pressing need for research. The integration of formal safety assuring methods like the control barrier functions becomes pivotal in developing safety-critical controllers, addressing a critical gap in autonomous vehicle overtaking.

1.2. Our contributions

Our work aims to address the gap between the present non-verifiable and error-prone control designs for overtaking control systems in autonomous driving and the increasing needs for safety guarantees. Specifically, we consider a challenging two-way overtaking scenario that includes possible opposite vehicles, as illustrated in Figure 1. To tackle this problem, we develop a novel framework that integrates the theories of varying-level control barrier functions (CBF) and time-optimal model predictive control (MPC). The main feature of our proposed overtaking strategy is that it is *safe-by-construction*, meaning that we can mathematically prove its safety guarantees. This approach eliminates the need for the possible tedious subsequential test-and-redesign cycle that often arises when formal methods are not used.

More specifically, the main contributions of this paper are summarised as follows:

- Firstly, we introduce a novel concept, referred to as varying-level control barrier functions (VL-CBF), which offers adjustable level sets. Unlike conventional CBFs that operate with fixed zero super-level sets, our novel VL-CBFs offer a dynamic and adjustable approach. This innovation is especially suitable for autonomous driving applications, as it allows for the integration of driver preferences and facilitates online adaptation of crucial parameters.
- Secondly, we present an integrated framework that combines the proposed VL-CBF with model predictive control for vehicle overtaking in a more complex scenario that includes potential opposing traffic. Notably, our framework addresses the complexity of the task by solving two optimisation problems at each time instant. The first pertains to forward overtaking of the front vehicle, while the second involves planning a trajectory for backward movement to the original position when the former problem proves unsolvable.
- We show that our proposed framework guarantees safety for the vehicles involved, and we formally establish this by first mathematically proving that our VL-CBF can enforce an arbitrary user-defined super-level set, then illustrating that at each instant, either the forward or the backward problem in our framework has a solution. Additionally, we show that the planned trajectories and associated control laws effectively avert collisions between the ego vehicle and both the front and the opposing vehicles. A set of simulations are also conducted to demonstrate the effectiveness of our results.

1.3. Related works

1.3.1. Autonomous overtaking manoeuvres

The increasing computational power has led to a rapid development of on-road overtaking controllers in the past years (Dixit et al., 2019; Milanés et al., 2012; Xie et al., 2022). Approaches in the literature for tackling the vehicle overtaking problem can be broadly categorised into three types: traditional model-based methods, data-driven methods and learning-based methods. For example, in Petrov and Nashashibi (2014), introduced a three-phase overtaking model which decomposes the overtaking actions into consecutive LC, LK and LC sub-problems, then using a kinematic model-based adaptive controller to solve the overall problem. This approach works under a simple scenario without surrounding traffic. In Diaz Alonso et al. (2008), Chae and Yi (2020), the authors used extended Kalman filters to estimate the vehicle states in order to switch between LC and LK modes.

Researchers have also devised data-driven approaches to formulate control laws by leveraging data gathered from expert drivers and simulations (Do et al., 2017; Li, Tan et al., 2020; Naranjo et al., 2008; Wang et al., 2017). In the case of Wang et al. (2017), vehicle trajectories are generated using a fuzzy inference system developed with naturalistic driving data to compute the dangerous level. Additionally, mathematical state estimation methods such as those in Luo et al. (2021), Luo, Wang, Sheng et al. (2023), are integrated with complex networks to provide state estimation. For the two-segment lane change controller proposed in Do et al. (2017), its aim is to emulate human-driver behaviour. However, the accuracy of these methods heavily depends on the quality of the data sets and lacks robust safety guarantees.

Learning-based planning methods with safety considerations have also been proposed recently in Liu et al. (2022, 2023). For example, in Liu et al. (2023), the authors proposed a neural network-based LC controller that leverages a back-up strategy to enhance safety. The readers are referred to Chen et al. (2021) for more planning methods within the end-to-end training framework.

Reinforcement learning techniques have also been used to perform overtaking tasks in partially-known or unknown environments (Li, Qiu et al., 2020; Liang et al., 2018; Ngai & Yung, 2011). For example, Rosolia and Borrelli (2020) proposed a deep learning-based race strategy by combining with MPC controllers. Since learning-based methods can hardly cover all possible scenarios that may happen on road due to the nature of their finite training data, they still cannot provide formal safety guarantees for overtaking tasks.

1.3.2. CBF-based vehicle control with formal guarantees

In recent years, control barrier functions (CBFs) have emerged as a highly successful technique for ensuring the safety of autonomous systems with formal guarantees (Ames et al., 2019). The fundamental principle of CBFs is to represent the safety of the system using a super-level set, the forward invariance of which can be enforced through constraints on the control inputs (Ames et al., 2019). The key idea is to define a value function that quantifies the distance to a safe set of states, such that it decreases as the system moves towards the safe set and increases otherwise. By incorporating this CBF into control design, one can ensure that the system remains within a predefined safe region. In the pioneering work by Ames et al. (2017), quadratic programming (QP) was applied to CBF, which made CBF computationally feasible for real-time control. To address various challenges in system design, many variants of CBFs have been proposed recently. For example, exponential CBF and high-order CBF have been developed to overcome the non-existence of first-order Lie derivatives (Nguyen & Sreenath, 2016; Xiao & Belta, 2022). Feasibility and discretization issues have been addressed in the literature, with works such as (Agrawal & Sreenath, 2017; Choi et al., 2021; Xiao et al., 2022a; Xiong et al., 2022). Additionally, observation-based CBFs (Dawson et al., 2022) and decentralised CBFs (Qin et al., 2021) have been proposed to extend the generality and scalability for large-scale systems in unknown environments. Barrier functions have also been utilised to enhance safety for learning-based controllers; see, e.g. Wang et al. (2023), Xiao et al. (2022c), Yang et al. (2023). In Wang et al. (2023), the authors proposed a joint differentiable optimisation and verification framework that can synthesise controllers and their certificates simultaneously. In Xiao et al. (2022c), Yang et al. (2023), CBFs are used as an add-on layer to neural network-based controllers to ensure safety.

In the specific context of autonomous vehicles, CBFs have been successfully applied to ensure safety for four categories of basic tasks. For instance, Xu et al. designed a composed CBF through a contract-based method that provided safety guarantees for simultaneous LK and ACC (Xu et al., 2018). Lyu et al. focussed on safe ramp merging cases, proposing a probabilistic CBF control law under Gaussian uncertainty of motion (Lyu et al., 2022). Furthermore, in Lyu et al. (2021), the authors developed an adaptive CBF learning structure for the ego vehicle based on the observation of others. Particularly, for the vehicle overtaking problems, He et al. proposed a rule-based three-phase overtaking framework using a finite state machine (FSM) to switch between different CBFs during different overtaking phases (He et al., 2021). The authors also proposed a race car overtaking strategy that combines CBF with a learning-based MPC method (He et al., 2022), enabling safe competition with surrounding vehicles on a closed track. While

these works provide basic solutions for formal safety guarantees in overtaking problems, it should be noted that the frameworks are developed only for simple scenarios without possible opposing traffic. For practical purposes, it is necessary to take unexpected opposing vehicles into account to ensure safety.

1.3.3. Challenges in overtaking with opposing vehicles

As we discussed above, most existing works on autonomous overtaking do not provide formal safety guarantees for the entire process except (He et al., 2021, 2022). While for He et al. (2021, 2022), they primarily focus on overtaking scenarios *without* opposing vehicles. Notably, these scenarios are inherently less complex than the case with opposing vehicles as we consider in this work. Specifically, without opposing vehicles, the completion of the overtaking task can be postponed indefinitely, allowing the ego vehicle to remain in the adjacent lane. However, in the presence of opposing vehicles, the optimisation problem has to be solved within a finite horizon since the opposing vehicle is approaching towards the ego vehicle. Therefore, we need to provide the estimated time for accomplishing the overtaking task with safety guarantees. Furthermore, the presence of opposing vehicle may make the overtaking task infeasible, and therefore, we also need to provide a back-up plan for safely returning to the original point. All these issues have not been considered in the literature, and our work seeks to bridge this gap by proposing an integrated method that addresses these challenges comprehensively.

1.4. Paper organisations

The paper is organised as follows. Section 2 formulates the two-way road overtaking problem. Section 3 revisits the theory of control barrier functions, and introduces the model we use in this study. Section 4 proposes the varying-level control barrier functions and investigates its related properties. Section 5 introduces our framework for two-way road overtaking, and establishes the formal guarantee for safety. Section 6 provides a set of simulations to illustrate the proposed approach, and gives comparison of the baseline method. Finally, Section 7 summarises the paper and discusses some future directions.

2. Problem formulation

In this paper, we focus on an overtaking scenario on a two-way road as depicted in Figure 1. Specifically, the current lane with the same traffic direction is denoted by $\mathcal{L}_{\text{ego}}$ and the opposing lane with the opposite traffic direction is denoted by $\mathcal{L}_{\text{opp}}$. We term our controlled vehicle as the *ego vehicle* (shown in green), denoted as veh_e; the front overtaken vehicle termed as *overtaken vehicle* (shown in red), denoted as veh_f, where f stands for 'front'; and the possible opposing vehicle (shown in blue) is denoted as veh_o.

Our objective is to design an *overtaking control strategy* for the ego vehicle veh_e with *provable safety guarantees*. Specifically, we require that:

- The ego vehicle veh_e can safely overtake the front vehicle veh_f by temporarily occupying the opposite lane $\mathcal{L}_{\text{opp}}$, while ensuring collision avoidance with both veh_f and the opposing vehicle veh_o if the overtaking task is feasible.
- If the overtaking task is not feasible, then ego vehicle veh_e must be able to return to its original position in $\mathcal{L}_{\text{ego}}$ safely ensuring collision avoidance with other vehicles.
- A formal guarantee can be established for collision avoidance and solution feasibilities throughout the entire overtaking process.

Remark 2.1: For the sake of simplicity and without loss of generality, in our later developments, we make the following assumptions regarding the behaviours of the front vehicle veh_f and the opposing vehicle veh_o.

- For the front vehicle veh_f, we assume that it is non-accelerating during the overtaking process. This assumption is reasonable for a rational driving scenario. In fact, our approach can be extended to the case, where veh_f is accelerating or non-accelerating but not interchangeably.
- For the opposing vehicle veh_o, our main analysis will be based on the assumption that it is also autonomous following the same safety-critical control law. This assumption enables us to perform a thorough analysis. When the opposing vehicle is driven by a human driver, we will also discuss using conservative analysis to address any deviations from our assumptions in Section 5.

3. Preliminaries

3.1. Vehicle models

In this work, the general dynamics of vehicles are described by the following nonlinear control affine model:

$$\dot{\mathbf{x}} = f(\mathbf{x}) + g(\mathbf{x})\mathbf{u}, \tag{1}$$

where $\mathbf{x} \in \mathcal{X} \subset \mathbb{R}^n$, and $\mathbf{u} \in \mathcal{U} \subset \mathbb{R}^m$ are the system state and control input, respectively, with $\mathcal{X}$ and $\mathcal{U}$ be the state and control constraints. Mappings f and g are both assumed to be Lipschitz continuous. For any initial condition $\mathbf{x}(0) \in \mathbb{R}^n$, there exists a maximum time interval $\mathcal{I}_{\max} := [0, \tau_{\max})$ such that $\mathbf{x}(t)$ is the unique solution to (1) on $\mathcal{I}_{\max}$.

More specifically, for the ego vehicle, we consider a precise non-holonomic kinematic bicycle model (Kong et al., 2015), which can be transferred into the following control affine model (He et al., 2021):

$$\dot{\mathbf{x}} = \begin{bmatrix} \dot{x} \\ \dot{y} \\ \dot{\psi} \\ \dot{v} \end{bmatrix} = \begin{bmatrix} v\cos\psi \\ v\sin\psi \\ 0 \\ 0 \end{bmatrix} + \begin{bmatrix} 0 & -v\sin\psi \\ 0 & v\cos\psi \\ 0 & \frac{v}{l_r} \\ 1 & 0 \end{bmatrix} \begin{bmatrix} \alpha \\ \beta \end{bmatrix}, \tag{2}$$

where $\mathbf{x} = [x, y, \psi, v]^\top$ denotes the state of the vehicle and $\mathbf{u} = [\alpha, \beta]^\top$ denotes the input of the vehicle with α be the acceleration at vehicle's center of gravity (c.g.) and β be the slip angle of the vehicle. The system states x, y are the longitudinal and lateral positions of the c.g. with respect to the inertial frame, respectively, and ψ, v represent the orientation and forward velocity of the vehicle, respectively. In the rest of this paper, we will use normal letter and bold letter to represent scalar and vector, respectively.

For the overtaken and opposing vehicles, lateral movements are negligible during the overtaking process, and only longitudinal behaviours are of our interest. Therefore, we use a simpler double integral model described as follows:

$$\dot{\mathbf{x}} = \begin{bmatrix} \dot{x} \\ \dot{v} \end{bmatrix} = \begin{bmatrix} 0 & 1 \\ 0 & 0 \end{bmatrix} \begin{bmatrix} x \\ v \end{bmatrix} + \begin{bmatrix} 0 \\ 1 \end{bmatrix} \alpha, \tag{3}$$

where α represents the along-road longitudinal acceleration rate of the double integral model.

3.2. Control barrier functions

Control barrier functions (CBFs) are recently developed successful techniques for ensuring safety for constrained control systems (Ames et al., 2017, 2019, Xiao et al., 2022b). The motivation to incorporate CBF into the autonomous driving system is that, without the need to calculate a safe reachable set through complex computations (Herbert et al., 2021), CBF imposes a linear constraint on the control input for control affine systems, enabling fast computation that can be carried out in real-time. Safety can be formally guaranteed through the forward invariance of the system states in a super-level set. Following the definition in Ames et al. (2017), we define the *safe set* $\mathcal{C}$ of the system as represented by the super-level set of a time-varying, continuously differentiable function $h(\mathbf{x}, t)$, where h quantifies the safety level of the system and can vary based on different safety requirements. Particularly, in our overtaking problem, the formulation of h is presented in (12) and (20). To ensure collision-free scenarios, we aim for this value function $h(\mathbf{x}, t)$ to be greater than 0; thus, the *safe set* is expressed as

$$\mathcal{C}(t) := \{\mathbf{x} \in \mathbb{R}^n : h(\mathbf{x}, t) \geq 0\}. \tag{4}$$

Note that when the control law $\mathbf{u} := k(\mathbf{x})$ is locally Lipschitz continuous, the control affine model $\dot{\mathbf{x}} = f(\mathbf{x}) + g(\mathbf{x})k(\mathbf{x})$ is still locally Lipschitz continuous. Therefore, for any initial condition $\mathbf{x}(0) \in \mathcal{C}(0)$, system (1) always has a unique solution within a time interval. The safety of the system is defined by the following forward invariance property.

Definition 3.1 (Forward Invariance and Safety (Xiao & Belta, 2022)): The set $\mathcal{C}$ is said to be *forward invariant* for a given control law $\mathbf{u}$ if for every $\mathbf{x}(0) \in \mathcal{C}(0)$, we have $\mathbf{x}(t) \in \mathcal{C}(t)$ holds for all $t \in [0, \tau_{\max})$, where $\mathbf{x}(t)$ is the unique solution to (1) starting from $\mathbf{x}(0)$. We say the system is *safe* if safe set $\mathcal{C}$ is forward invariant.

We use the concept of control barrier functions to characterise the admissible set of control inputs that guarantee the set $\mathcal{C}$ is forward invariant. Recall that a continuous function $\kappa : (-b, a) \to (-\infty, \infty)$ for $a, b \in \mathbb{R}_{\geq 0}$ belongs to the extended class of $\mathcal{K}$ functions (also called class $\mathcal{K}_e$ functions) if it is monotonically increasing and satisfies $\kappa(0) = 0$ (Khalil, 2015). Now we introduce the definition of CBF as follows.

Definition 3.2 (Control Barrier Functions (Ames et al., 2017)): Let $h(\mathbf{x}, t) : \mathbb{R}^n \times \mathcal{I}_{\max} \to \mathbb{R}$ be a continuously differentiable function. We say h is a *control barrier function* for system (1) if there exists a class $\mathcal{K}_e$ function $\kappa(\cdot)$ such that

$$\sup_{\mathbf{u}\in\mathcal{U}} \left[L_f h(\mathbf{x}, t) + L_g h(\mathbf{x}, t)\mathbf{u} + \frac{\partial h}{\partial t} \right] \geq -\kappa(h(\mathbf{x}, t)), \tag{5}$$

for all $(\mathbf{x}, t) \in \mathcal{C}(t) \times \mathcal{I}_{\max}$, where $L_f h(\mathbf{x}, t) \coloneqq \frac{\partial h(\mathbf{x},t)^\top}{\partial \mathbf{x}} f(\mathbf{x})$ and $L_g h(\mathbf{x}, t) \coloneqq \frac{\partial h(\mathbf{x},t)^\top}{\partial \mathbf{x}} g(\mathbf{x})$ are the Lie derivatives.

Similar to the application of Lyapunov functions to certify stability properties without the need for exact solution calculations, the concept of control barrier functions aims to establish the forward invariance of a safe set, without the intricate computation of the system's reachable tube. In (5), the left-hand side essentially represents the total derivative $\dot{h}$ of the value function h, and this leads to

$$\dot{h}(\mathbf{x}, t) \geq -\kappa \circ h(\mathbf{x}, t), \quad \forall (\mathbf{x}, t) \in \mathcal{C}(t) \times \mathcal{I}_{\max}. \tag{6}$$

Adhering to Nagumo's principle (Blanchini, 1999), the set $\mathcal{C}(t)$ in (4) is forward invariant. Consequently, for any control input satisfying (5), it ensures the forward invariance of the state who renders the value function $h(\mathbf{x}, t) \geq 0$.

Given a CBF $h(\mathbf{x}, t)$, we formally write the set of all control values that render set $\mathcal{C}$ safe by

$$K_{\text{cbf}}(\mathbf{x}, t) \coloneqq \left\{ \mathbf{u} \in \mathcal{U} : L_f h + L_g h\mathbf{u} + \frac{\partial h}{\partial t} + \kappa(h) \geq 0 \right\}, \tag{7}$$

which denotes the safe control input set. The following theorem shows that the existence of a CBF can provide formal safety guarantee for the system.

Lemma 3.1 (Corollary 2 (Ames et al., 2017)): *Let $h(\mathbf{x}, t)$ be a valid CBF and assume that $\frac{\partial h(\mathbf{x},t)}{\partial \mathbf{x}} \neq \mathbf{0}^n$ for all $(\mathbf{x}, t) \in \partial\mathcal{C}(t) \times \mathcal{I}_{\max} \subset \mathbb{R}^n \times \mathbb{R}$. Then any Lipschitz continuous controller $\mathbf{u} \coloneqq k(\mathbf{x})$ such that $\mathbf{u} \in K_{\text{cbf}}(\mathbf{x}, t)$ for every $(\mathbf{x}, t) \in \mathcal{C}(t) \times \mathcal{I}_{\max}$ will render set $\mathcal{C}$ forward invariant.*

For control affine systems in (1), K_{cbf} in (7) leads to linear constraints on control inputs, which can be incorporated into computationally tractable QP-based controllers (Ames et al., 2017). When incorporating different driving preferences in on-road overtaking scenarios, conventional methods require us to redesign h case-by-case, whereas we introduce our VL-CBF method to provide adjustable level set of h in the next section.

4. Varying-level control barrier functions

In the preceding section, we presented a fundamental definition of control barrier functions as a crucial tool for ensuring safety. In this section, we introduce a novel concept called *Varying-Level Control Barrier Functions*. This concept is aimed at improving the explanatory power and user parametrisation capabilities of CBFs.

4.1. Varying-level control barrier functions

Note that Definition 3.2 for CBF only requires the existence of a $\mathcal{K}_e$ function $\kappa(\cdot)$ for h. Different functions inherently correspond to distinct autonomous system behaviour patterns. In autonomous driving, control laws must characterise user-defined diverse behaviour patterns and be explainable. To this end, the concept of parametric CBF (PCBF) was proposed in Lyu et al. (2022) to capture these requirements, where the function $\kappa(\cdot)$ is restricted to a polynomial with odd powers of h. The coefficients in the polynomial provide parameters for the driver to choose, achieving the purpose of user-defined diverse behaviour patterns.

However, PCBF can only enforce the *zero super-level set* as described in (4). As value function $h(\mathbf{x}, t)$ is typically selected as the distance between two vehicles, enforcement of the zero super-level set essentially means that two vehicles can be arbitrarily close, as long as they do not collide. In practice, drivers are more conservative and want to enforce a *positive super-level set* of $h(\mathbf{x}, t)$. This conservative degree should also be parameterised, so that each user can choose their safety margin. To this end, motivated by the existing PCBF, we propose the following VL-CBF.

Definition 4.1 (Varying-Level Control Barrier Functions): Given a dynamic system model as in (1), and the nominal safe set $\mathcal{C}(t)$ defined as (4) with time-varying differentiable value function $h(\mathbf{x}, t) : \mathbb{R}^n \times \mathcal{I}_{\max} \to \mathbb{R}$. Then h is said to be a varying-level control barrier function (VL-CBF) of order $m \geq 1$ if

$$\sup_{\mathbf{u}\in\mathcal{U}} [L_f h(\mathbf{x}, t) + L_g h(\mathbf{x}, t)\mathbf{u} + \frac{\partial h(\mathbf{x}, t)}{\partial t}] \geq -\Lambda H(\mathbf{x}, t), \tag{8}$$

holds for all $(\mathbf{x},t)\in\mathcal{C}(t)\times\mathcal{I}_{\max}$, where $\Lambda\coloneqq[\lambda_0,\lambda_1,\ldots,\lambda_m]\in\mathbb{R}^{m+1}$ and $H(\mathbf{x},t)\coloneqq[1,h,h^3,h^5,\ldots,h^{2m-1}]^\top$ such that $\Lambda H(\mathbf{x},t)$ is a polynomial equation consists of a constant and odd powers of h.

The purpose of defining VL-CBF is to enforce an arbitrary driver-defined non-negative super-level set

$$\mathcal{C}_\epsilon(t)\coloneqq\{x\in\mathcal{X}:h(\mathbf{x},t)\geq\epsilon\},\tag{9}$$

such that more conservative safety requirement can be fulfilled. Similar to the case of standard CBF, we define

$$K_{\text{vlcbf}}(\mathbf{x},t)\coloneqq\left\{\mathbf{u}\in\mathcal{U}:L_fh+L_gh\mathbf{u}+\frac{\partial h}{\partial t}+\Lambda H\geq 0\right\}\tag{10}$$

as the set of safe control inputs. Then the following result shows that this purpose can be achieved by suitably choosing a negative parameter λ_0, which will be referred to as the *level parameter*, in Λ.

Theorem 4.1: *Let $h(\mathbf{x},t)$ be a valid VL-CBF, and assume that $\frac{\partial h}{\partial\mathbf{x}}\neq\mathbf{0}^n$ for all $(\mathbf{x},t)\in\partial\mathcal{C}(t)\times\mathcal{I}_{\max}\subset\mathbb{R}^n\times\mathbb{R}$. Then for any $\epsilon\in\mathbb{R}_{\geq 0}$ there exists a set of parameter Λ, where the level parameter $\lambda_0\in\mathbb{R}_{\leq 0}$, and $\lambda_i\in\mathbb{R}_{\geq 0}$ for $i\in\{1,\ldots,m\}$, such that any Lipschitz continuous controller satisfying $\mathbf{u}\in K_{\text{vlcbf}}(\mathbf{x},t)$ for every $(\mathbf{x},t)\in\mathcal{C}_\epsilon(t)\times\mathcal{I}_{\max}$ will render set $\mathcal{C}_\epsilon$ forward invariant.*

Proof: We define $\tilde{\kappa}(h)\coloneqq[\lambda_1,\ldots,\lambda_m][h,\ldots,h^{2m-1}]^\top$, which is a polynomial sum starting from the second term of the polynomial equation ΛH. As proved in Lyu et al. (2022), $\tilde{\kappa}(h)$ is a class $\mathcal{K}_e$ function of h. Using this new notation, (8) can be rewritten as

$$L_fh+L_gh\mathbf{u}+\frac{\partial h}{\partial t}\geq-\lambda_0-\tilde{\kappa}(h),\tag{11}$$

where the right hand side of the equation consists of a class $\mathcal{K}_e$ function and a level parameter λ_0. For any $\epsilon\in\mathbb{R}_{\geq 0}$, the initial condition $\mathbf{x}(0)\in\mathcal{C}_\epsilon(0)$ implies $h(\mathbf{x}(0),0)\geq\epsilon$, then we show that there always exists a λ_0 that can render $\mathcal{C}_\epsilon$ forward invariant.

Let $\lambda_0=-\tilde{\kappa}(\epsilon)\in\mathbb{R}_{\leq 0}$, through (11) we have $\dot{h}\geq\tilde{\kappa}(\epsilon)-\tilde{\kappa}(h)$ for all $t\in\mathcal{I}_{\max}$ whenever $h>\epsilon$, which suggests the value of h might decrease when h is greater than ϵ; whereas, when $h\to\epsilon$ we have $\dot{h}\geq 0$, suggesting the value of h cannot decrease further below ϵ. Thus $\forall\mathbf{x}(0)\in\mathcal{C}_\epsilon(0)$, we always have $h(\mathbf{x},t)\geq\epsilon,\forall t\in\mathcal{I}_{\max}$. This completes the proof. ■

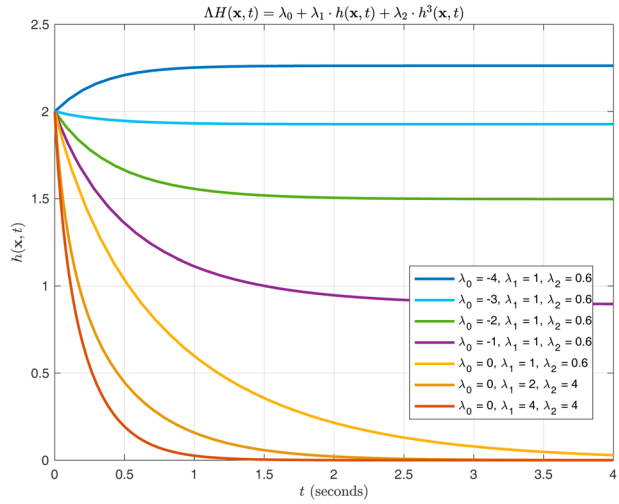

Figure 2. Arbitrary super-level set enforced by VL-CBF.

We demonstrate the varying level property as in Figure 2, where the value function h is chosen to be $h(\mathbf{x},t)\coloneqq x-x_d-\frac{v^2}{2a_{max}}$ where x_d is the position of the obstacle the system wants to avoid, and a_{max} is the maximum deceleration rate of the system, which is a simple case of (12) without other moving vehicles. As illustrated in Figure 2, we show a VL-CBF parameterised by three parameters $\Lambda=[\lambda_0,\lambda_1,\lambda_2]$, under the same value function h. Specifically, different choices of non-level parameters λ_1 and λ_2 yields different divergent horizons of its level set. Furthermore, when those non-level parameters are fixed, choosing a smaller level parameter λ_0 yields a higher the horizon of the super-level set for $h(\mathbf{x},t)$, which implies that a more conservative safety control strategy enforcing a positive super-level set. The top blue curve illustrates the case when the initial value for h is lower than the safety level, thus the value for h will rise from the beginning.

Remark 4.1: Note that the requirement of enforcing the ϵ-super-level set of h can also be achieved via the standard CBF by redefining function h. This is essentially a hand-coded approach, requiring a change in the underlying h for different ϵ. The key feature of the proposed VL-CBF is the ability to circumvent this manual coding. The level parameter λ_0 gives the system the ability to change the horizon of its super-level set for $h(\mathbf{x},t)$, without the need to redesign the original $h(\mathbf{x},t)$ for different conservativeness degrees. This setting makes more sense for decentralised autonomous

vehicle control, since under the identical safety criteria, each individual may have its own interpretation of the conservativeness towards the safety boundary.

4.2. Safety guarantees for two-way overtaking via VL-CBF

For the two-way road overtaking problem, it is crucial to guarantee that the ego vehicle (veh_o) does not collide with the opposing vehicle (veh_o) while traversing from $\mathcal{L}_{\text{ego}}$ into the opposing lane $\mathcal{L}_{\text{opp}}$. With the incorporation of the proposed VL-CBF, we demonstrate that the ego vehicle and the opposing vehicle can maintain safety, provided that the initial condition is satisfied.

Considering the longitudinal velocity of both vehicles, the value function that quantifies the collision-free safety criteria for the ego vehicle dynamics is expressed as:

$$h_{eo}(\mathbf{x}_e, t) \coloneqq x_o - x_e - \frac{(v_e^x - v_o^x)^2}{2a_l}, \tag{12}$$

where h_{eo} describes the worst-case physical condition of the final distance between each vehicle under the maximum deceleration rate (a_l). To meet the safety requirement of collision-free overtaking, this value function must be greater than 0.

For the opposing vehicle veh_o, by assuming that it is also autonomous and adopts VL-CBF, the safety condition is defined as

$$h_{oe}(\mathbf{x}_o, t) \coloneqq x_o - x_e - \frac{(v_e^x - v_o^x)^2}{2a_l}. \tag{13}$$

In the above equations, a_l is the maximum deceleration rate, and $\mathbf{x}_e, \mathbf{x}_o$ stand for the states of veh_e, veh_o respectively. We use x_e to represent the first element of $\mathbf{x}_e$ in (2) with $v_e^x \coloneqq \dot{x}_e$; similarly, x_o and v_o^x are two elements of $\mathbf{x}_o$ in (3). Furthermore, we introduce two symbols α_e^x, α_o^x which will be used later, with $\alpha_e^x \coloneqq \ddot{x}_e$ and α_o^x is the control input of the system as defined in Equation (3). Note that in Equations (12) and (13), x_o, v_o^x and x_e, v_e^x are time-varying parameters respectively. As shown in Equations (12) and (13), the value functions h_{eo} and h_{oe} have the same expression but different independent variables, suggesting that they have the same interpretation of their relative status.

The safety guarantee with respect to the opposing vehicle during the lane borrowing process is established as follows.

Theorem 4.2: *Consider VL-CBFs defined in Equations* (12) *and* (13)*, and assume that both veh_e and veh_o follow the safety control law defined in Equation* (10)*. Then if the initial safety condition $\Lambda_\times H_\times \geq 0,\ \forall \times \in \{eo, oe\}$ is satisfied, the collision-free solution exists for both vehicles under the control limits.*

Proof: As the value function defined as (12), (13), we have $H_{eo} = [1, h_{eo}, \ldots, h_{eo}^{2m-1}]$ and $H_{oe} = [1, h_{oe}, \ldots, h_{oe}^{2m-1}]$ sharing the same expression. For veh_e in $\mathcal{L}_{\text{ego}}$, to satisfy VL-CBF we have

$$\dot{h}_{eo} = v_o - v_e - \frac{2(v_e^x - v_o^x)(\alpha_e^x - \alpha_o^x)}{2a_l} \geq -\Lambda_{eo} H_{eo} \tag{14}$$

which yields

$$\alpha_e^x - \alpha_o^x \leq \frac{a_l}{v_e^x - v_o^x}(\Lambda_{eo} H_{eo} + v_o^x - v_e^x), \tag{15}$$

whereas for veh_o in the opposite direction, we have

$$\alpha_e^x - \alpha_o^x \leq \frac{a_l}{v_e^x - v_o^x}(\Lambda_{oe} H_{oe} + v_o^x - v_e^x). \tag{16}$$

We first show that for all the scenarios under VL-CBF, we can find a joint relation so that the safety can be preserved under the maximum deceleration limit a_l. We define a new variable $\mathcal{H} \coloneqq \min\{\Lambda_\times H_\times\}, \times \in \{eo, oe\}$, and by combining (15) and (16), we have

$$\alpha_e^x - \alpha_o^x \leq \frac{a_l \mathcal{H}}{v_e^x - v_o^x} - a_l. \tag{17}$$

To ensure the feasibility of the proposed barrier function, the right-hand side of (17) must be greater than the lowest possible value of the difference in controller value when $\alpha_e^x = -a_l, \alpha_o^x = a_l$. Note that, a_l is the absolute value of the maximum deceleration rate, which corresponds to vehicles decelerating at their extreme capacity. Thus, the following inequality must hold

$$\frac{a_l \mathcal{H}}{v_e^x - v_o^x} \geq -a_l. \tag{18}$$

Since $v_e^x - v_o^x > 0$ when v_e^x is positive and v_o^x is negative, the feasibility of this safety solution can be guaranteed if the two vehicles satisfy

$$\mathcal{H} + v_e^x - v_o^x \geq 0. \tag{19}$$

Satisfaction of (19) suggests the existence of the solution at least at their extreme control capability.

Then, we show that (19) holds if the initial condition is satisfied: we have $\mathcal{H} \geq 0$ as $\Lambda_\times H_\times \geq 0$ is fulfilled. Since $v_e^x - v_o^x$ is positive, it follows that the inequality in (19) is always satisfied, which indicates the feasibility of the original VL-CBF. According to Theorem 4.1, safety can be ensured by the invariant property of its super-level set. This completes the proof. ■

Remark 4.2: In the above result, the initial safety condition $\Lambda_\times H_\times$ defines a nominal safe margin for the vehicle, indicating the edge of the safe space under the conservativeness degree ϵ decided by $\Lambda_\times$. Note that, the system can further withstand disturbances by raising the VL-CBF level to increase conservativeness, and when $\lambda_0 = 0$, this initial condition simply indicates that under the maximum deceleration rate, the two vehicles can stop at the very last moment with the minimum conservative distance they defined, which is their physical limit at the most extreme situation.

5. Two-way road overtaking framework

In the preceding section, we have developed the basic tool of VL-CBF for ensuring safety in the presence of opposing vehicles. In this section, we present our overall overtaking framework, which can tackle both the front vehicle as well as the potential opposing vehicle. To present the integrated framework, we proceed in this section as follows:

- We begin by presenting the mathematical formulation of our approach, named time-optimal control barrier function-based model predictive Control (TO-CBF-MPC). This method combines time-optimal MPC with the previously introduced VL-CBF. The objective is to address the front vehicle overtaking problem. In this formulation, the time-optimal control problem is solved using MPC, leveraging the VL-CBF for safety guarantees.
- Then we introduce an integrated overtaking framework for dealing with the potential opposing traffic. Specifically, at each instant, we need to solve two safety-guarantee optimisation problems: one for overtaking the front vehicle and the other for returning to the original position. We prove that at least one of these two problems is always feasible, which provides a formal guarantees of safety for the overall framework.
- Finally, we discuss the extensibility of our framework to further incorporate the semi-autonomous surrounding vehicles with human drivers. We show how safety guarantees can still be ensured through conservative analysis.

5.1. CBF-based time-optimal model predictive control

First, we focus on the overtaking scenario only involving the front vehicle. We formulate this scenario as a time-optimal control problem with safety constraints. Specifically, we solve this problem using model predictive control (MPC) whose objective function is to minimise the overtaking time yet maintaining a safe distance from the front vehicle, together with other constraints to consider the vehicle dynamics and performance factors.

In order to efficiently handle the safety requirement with respect to the front overtaken vehicle, VL-CBF is used as a constraint in the optimisation problem. As shown in Figure 3, we model the safety requirement with respect to the front vehicle by an ellipse that covers the front vehicle, where a, b are the radius of the ellipse. Let x_f and y_f be the longitudinal and lateral states of the front overtaken vehicle, respectively, and we denote $\mathbf{x}_f = [x_f, y_f]$. $\mathbf{x}_e$ is used as Section 4 to denote the state of the ego vehicle. We define a (VL-)CBF

$$h_{ef}(\mathbf{x}_e, t) \coloneqq \beta_1 \|x_e(t) - x_f(t)\|^2 + \beta_2 \|y_e(t) - y_f(t)\|^2 - \beta_3, \tag{20}$$

where $\beta_i,\ i \in \{1, 2, 3\}$ are hyper-parameters satisfying $\beta_1/\beta_3 = a^2$ and $\beta_2/\beta_3 = b^2$. Then this CBF defines the desired ellipse safe region $\mathcal{C}^f$ with respect to the overtaken vehicle veh_f, i.e.

$$\mathcal{C}^f(t) \coloneqq \{\mathbf{x}_e \in \mathbb{R}^4 : h_{ef}(\mathbf{x}_e, t) \geq 0\}. \tag{21}$$

By incorporating the VL-CBF, the safety constraint on the control input $\mathbf{u}_e$ for overtaking veh_f becomes

$$L_f h_{ef} + L_g h_{ef} \mathbf{u}_e + \frac{\partial h_{ef}}{\partial t} \geq \Lambda_{ef} H_{ef}, \tag{22}$$

which resulting in a non-negative super-level set

$$\mathcal{C}_\epsilon^f(t) \coloneqq \{\mathbf{x}_e \in \mathbb{R}^4 : h(\mathbf{x}_e, t) \geq \epsilon\}, \tag{23}$$

with $\epsilon \in \mathbb{R}_{\geq 0}$.

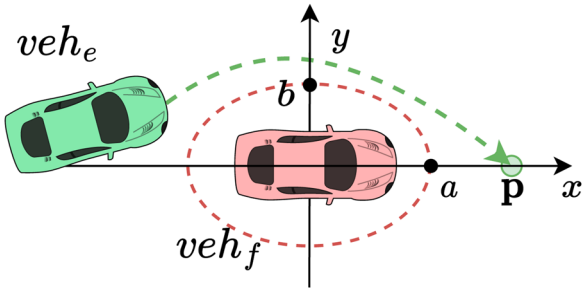

Figure 3. Relative ellipse around the front overtaken vehicle.

We formally introduce the time-optimal control barrier function-based model predictive control problem, denoted as TO-CBF-MPC. The optimisation problem is defined over a prediction horizon N encompassing the entire optimisation steps. Then the problem is formulated as follows:

- The decision variables consist of a trajectory $\{\mathbf{x}_e\}^N$ of the ego vehicle, a control input sequence $\{\mathbf{u}\}_e^N$ and a sequence of time intervals $\{\Delta t\}^N$. We denote by $\mathbf{x}_e^i$, $\mathbf{u}_e^i$ and Δt_i the ith entries in $\{\mathbf{x}_e\}^N$, $\{\mathbf{u}_e\}^N$ and $\{\Delta t\}^N$ respectively. Then Δt_i is the time interval between states $\mathbf{x}_e^i$ and $\mathbf{x}_e^{i+1}$ within which control input $\mathbf{u}_e^i$ is applied. Their relations are captured by the constraints in Equations (24b), (24c) and (24d). Furthermore, Equations (24e) put constraint on the maximum time interval between each intermediate point in order to mitigate the inter-sampling effect (Xiao et al., 2022c).
- The terminal constraint of the trajectory is captured by Equations (24f) and (24g). A reference goal location $\mathbf{p} = [x_g, y_g]$ is chosen in front of the overtaken vehicle in its longitudinal direction. The lateral bias parameter ϵ_y limits the optimised final position. Here, x_g is determined based on the speed and reaction time of the front vehicle veh_f, typically computed as $x_g = x_f + \phi v_f(t)$, with ϕ representing the reaction time (usually takes 1.8 s (Xiao et al., 2022c)).
- The safety constraint for the front vehicle (or surrounding vehicle during the overtaking process) is captured by Equation (24h), which is a VL-CBF constraint that ensures all planned states $\{\mathbf{x}\}^N$ are collision-free with minimum clearance to the ellipse defined in (21) of $\tilde{\kappa}^{-1}(\lambda_0)$, where $\tilde{\kappa}^{-1}$ is the inverse function of $\tilde{\kappa}$ in Theorem 4.1, and λ_0 here is the first element of Λ_{ef} in (24h).
- The overall optimisation objective is to estimate and minimise the total time taken before reaching the goal location, expressed as $\sum_{i=0}^{N-1} \Delta t_i$. Thus, the optimisation result also provides an *estimated time* for completing the overtaking task.

TO-CBF-MPC:

$$\min_{\{\mathbf{u}_e\}^N \in \mathcal{U}^N, \{\mathbf{x}_e\}^N \in \mathcal{X}^N, \{\Delta t\}^N} J = \sum_{i=0}^{N-1} \Delta t_i$$

subject to (24a)

$$\mathbf{x}_e^{i+1} = f(\mathbf{x}_e^i) + g(\mathbf{x}_e^i)\mathbf{u}_e^i \Delta t_i, \quad i \in \{0, \ldots, N-1\} \tag{24b}$$

$$\mathbf{u}_e^i \in \mathcal{U}, \quad i \in \{0, \ldots, N-1\} \tag{24c}$$

$$\mathbf{x}_e^i \in \mathcal{X}, \quad i \in \{0, \ldots, N-1\} \tag{24d}$$

$$\Delta t_i \leq t_{max}, \quad i \in \{0, \ldots, N-1\} \tag{24e}$$

$$x_e^N \geq x_g \tag{24f}$$

$$y_e^N \in [y_g - \epsilon_y, y_g + \epsilon_y], \quad \epsilon_y > 0 \tag{24g}$$

$$L_f h_{ef}^t + L_g h_{ef}^t \mathbf{u}_e^i + \frac{\partial h_{ef}^t}{\partial t} \geq -\Lambda_{ef} H_{ef}^t, \quad i \in \{0, \ldots, N-1\} \tag{24h}$$

Note that when applying MPC-based control, the above optimisation problem needs to be solved iteratively based on the current actual state. Specifically, for each time instant, only the first control entry $\mathbf{u}_e^0 \in \{\mathbf{u}_e\}^N$ in the computed input sequence is applied. The control input will be updated when the next optimisation problem is solved. Then at the start of next iteration, we re-measure the states of veh_e and veh_f, and re-compute $\{\mathbf{u}_e\}^N$ by solving TO-CBF-MPC, still apply its control entry, and so forth. The convergence criteria is met when the first state $\mathbf{x}_e^0$ at the next iteration satisfies the relationships $x_e^0 \geq x_g$ and $y_e^0 \in [y_g - \epsilon_y, y_g + \epsilon_y]$, which are analogue to Equations (24f) and (24g).

Remark 5.1: It is worth remarking that the safe-by-construction property of our solution is ensured by the VL-CBF constraint and it is independent from the objective function in the optimisation problem. In the proposed TO-CBF-MPC approach, we only consider the overtaking time as the single objective function to simplify the setting. Importantly, this simplification does not compromise generality, as any additional user-preferred performance metric can be added to the

objective function without affecting the overall safety property. For example, if one wants to further limit the changing rate of the acceleration to smooth the driving behaviour, then $\frac{\gamma_{\mathbf{u}}}{N}\sum||\mathbf{u}_e^{i+1}-\mathbf{u}_e^i||, i\in\{0,\dots,N-1\}$ can be added to the objective function with $\gamma_{\mathbf{u}}\geq 0$ as a user-defined weight (Althoff et al., 2021).

5.2. Integrated overall overtaking framework

With the previously introduced TO-CBF-MPC for motion planning and overtaking time estimation, we now consider the scenario when opposing traffic occurs while we are still borrowing the opposite lane. In this case, we need to consider the possible position of veh_o within the time horizon $\{x_o\}^N$ to safely plan our motion via the above TO-CBF-MPC.

Still, we assume that veh_o is autonomous and follows a (possibly non-identical) VL-CBF control law whose parameters Λ_o can be obtained by the ego vehicle veh_o via, for example, communications. Then by knowing parameters Λ_o, the ego vehicle can precisely estimate the control upper bound of the opposing vehicle when driving towards it. Therefore, when solving the TO-CBF-MPC problem, the following constraints need to be added into (24) in order to ensure safety with respect to the opposing vehicle

$$\mathbf{x}_o^{i+1}=f_o(\mathbf{x}_o^i)+g_o(\mathbf{x}_o^i)\mathbf{u}_o^i\Delta t_i \tag{25a}$$

$$L_f h_{eo}^t+L_g h_{eo}^t\mathbf{u}_e^i+\frac{\partial h_{eo}^t}{\partial t}\geq-\Lambda_{eo}H_{eo}^t \tag{25b}$$

$$L_{f_o} h_{oe}^t+L_{g_o} h_{oe}^t\mathbf{u}_o^i+\frac{\partial h_{oe}^t}{\partial t}\geq-\Lambda_{oe}H_{eo}^t, \tag{25c}$$

for $i\in\{0,\dots,N-1\}$, where (25a) is the dynamic for veh_o in (3). Then, after incorporating the new VL-CBF constraints above, we can jointly get the estimated sequence of $\{\mathbf{x}_e\}^N,\{\mathbf{u}_e\}^N,\{\mathbf{x}_o\}^N,\{\mathbf{u}_o\}^N$ within the prediction horizon, as well as the sequence of intervals $\{\Delta_t\}^N$ between time steps. Since VL-CBF (25c) regulates the most radical behaviour possible of veh_o, by solving the re-formulated TO-CBF-MPC problem, the resulting control action is collision-free to both veh_f and veh_o by construction, which is formally stated by the following result.

Theorem 5.1: *Suppose veh_f is non-accelerating during the overtaking process, the proposed overtaking control strategy is safe for the ego vehicle as long as the initial feasibility of the incorporated TO-CBF-MPC problem is satisfied.*

Proof: The initial feasibility of the above optimisation problem ensures the solution exists under current velocity of veh_f, and the potential autonomous opposing traffic, and therefore, the safety is always preserved under the longitudinal and ellipse-shaped VL-CBFs. And since veh_f is non-accelerating, the actual time taken to overtake the veh_f ($\sum\Delta\bar{t}_i$) will be less than or equal to the planned overtaking time $\sum\Delta t_i$, as we consider the relative position and velocity w.r.t. veh_e. Thus, the overtaking can be completed with less time taken, suggesting that the constraint in (24e) will always be satisfied, and the system can accept smaller control input $\mathbf{u}$ that being contained in the original solution space. This completes the proof. ■

Remark 5.2: The developments of our framework are based on the assumption that the strategy of the opposing vehicle is known to the ego vehicle. When this assumption does not hold, our framework can still be applied by further leveraging some techniques from the literature. One possible approach is to utilise the *parameter learning by interaction* technique in Lyu et al. (2022) that learns the driving parameters Λ_o through interactions on-the-fly. Another approach is to use the *conservative analysis* technique to estimate the worst-case of veh_o during the process. This approach is more general as it can be even applied to any possible control strategy for veh_o, but consequently, it also is more conservative. Details on how this conservative analysis can be integrated into our framework is provided in Section 5.3.

The formal safety guarantee in Theorem 5.1 is based on the assumption that veh_f is cooperative in the sense that it is non-accelerating during the overtaking process. In practice, if veh_f is also accelerating, then overtaking task may not be feasible. In this scenario, the ego vehicle needs a mechanism to recognise this issue and to take defensive actions such as stopping the overtaking process.

To address the above issue, we introduce a *dual TO-CBF-MPC* structure which provides ego vehicle the option to back to $\mathcal{L}_{\text{ego}}$ when overtaking is not feasible. Our integrated two-way road overtaking strategy with dual TO-CBF-MPC structure is illustrated in Figure 5. Specifically, instead of solving a safe overtaking control problem, we further solve a safe control problem, where the goal is to return back to the front vehicle. Therefore, two different reference goal locations $\mathbf{p}_1=$

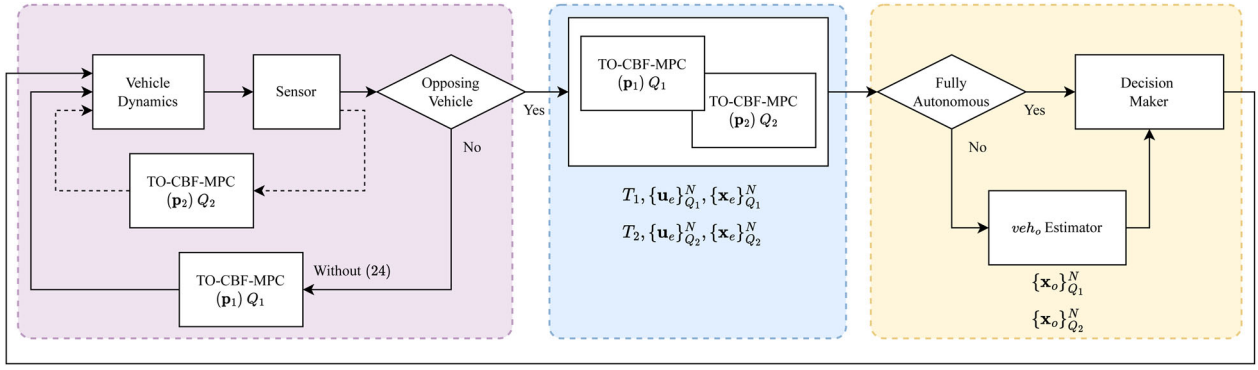

Figure 4. The two-way road overtaking framework considering opposing traffic. The framework consists of three parts (emphasised in the dashed colour blocks), where the left purple block depicts the control diagram when no opposing vehicle is around, the middle blue block depicts the *dual* TO-CBF-MPC mechanism for forward and backward planning, and the right yellow block depicts the switch to our decision maker for coping with human driver-based opposing vehicles.

$[x_g^1, y_g^1]$ and $\mathbf{p}_2 = [x_g^2, y_g^2]$ are selected, one in front of veh_f and the other behind veh_f, which correspond to two TO-CBF-MPC problems (with different $[x_g, y_g]$); we term the MPC problem from $[x_e, y_e]$ to $[x_g^1, y_g^1]$ as Q_1, and to $[x_g^2, y_g^2]$ as Q_2. To put it simply, Q_1 plans the actions to overtake veh_f, while Q_2 serves as a back-up strategy for this safety-critical system to abandon the overtaking process when the feasibility of overtaking is at risk.

At the beginning of the overtaking manoeuvre, the ego vehicle veh_e detects initial feasibility of Q_1, i.e. whether there is potential conflict when placing the reference goal location $\mathbf{p}_1$, and whether there exist opposing traffic that may cause unexpected danger (violates the initial conditions in Theorem 4.2). If the initial feasibility condition is fulfilled, then the overtaking manoeuvre begins. The proposed overtaking framework is illustrated in Figure 4. It starts by continuously detecting whether there exists opposing vehicle or not. If no opposing vehicle occurs, then it iterates through Q_1 by applying $\mathbf{u}^0$ at each iteration until convergence. After moving out of the current lane, Q_2 becomes active, with $\mathbf{p}_2$ as reference goal location relative to veh_f at its back. When Q_1 is unsolvable, e.g. due to the acceleration of veh_f, the system shifts toward the loop of Q_2, shown in the dashed-loop in Figure 4, and it will be guided back into its original lane. The following theorem shows that our framework ensures at least one MPC problem has a solution at each instant.

Theorem 5.2: *By adapting the integrated overtaking framework with the dual TO-CBF-MPC structure shown in Figure 4, at least one of the aforementioned TO-CBF-MPC problems Q_1, Q_2 is feasible during the overtaking process regardless of veh_f is accelerating or decelerating, but not interchangeably.*

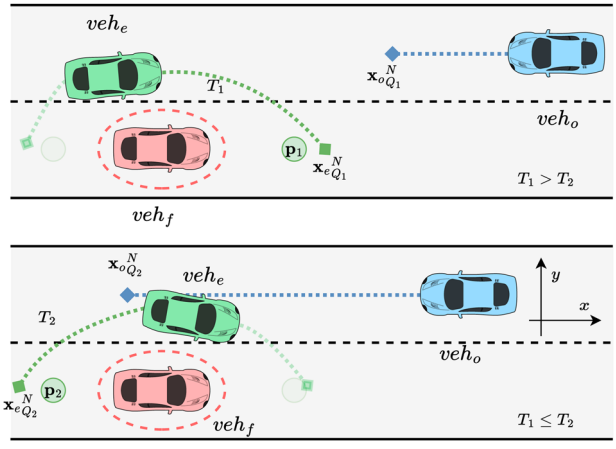

Figure 5. Illustration of the two-way road overtaking strategy. The upper figure shows the prediction process of the TO-CBF-MPC problem Q_1, where the green dotted line represents the estimated N points of veh_e's trajectory within the time T_1 to reach $\mathbf{p}_1$ and the blue dotted line represents the estimated veh_o's trajectory during this time. The lower figure shows the process of solving TO-CBF-MPC problem Q_2 when Q_1 is infeasible.

Proof: The start of the overtaking process suggests the satisfaction of the initial feasibility, which states that there exists solution to problem Q_1 and Q_2 so that $\mathbf{x}_e$ to $\mathbf{p}_1$ and $\mathbf{p}_2$ are feasible. For overtaking problem Q_1, the in-feasibility of (24) can only be affected by (24e), i.e. when $T_1 > Nt_{max}$. This corresponds to the case that veh_f accelerates when veh_e overtaking, which means the relative position and velocity of veh_f is beyond our initial measurements. We denote the predicted longitudinal distance between $\mathbf{x}_e$ and $\mathbf{p}_1, \mathbf{p}_2$ as l_x^1, l_x^2 respectively, then the violation of (24e) suggests that $\|x_e -$

$x_g^1\| > l_x^1$. Since $\mathbf{p}_1, \mathbf{p}_2$ is placed relative to the $\mathbf{x}_f$, it suggests $\|x_g^1 - x_g^2\| = c$, where c is a constant. Thus, for $\mathbf{x}_e$ to $\mathbf{p}_2$ we have $\|x_e - x_g^2\| < l_x^2$, resulting in a smaller relative distance in longitudinal direction; and since veh_f is accelerating, the relative velocity (acceleration) between veh_e and veh_f is also greater for Q_2, therefore, with shorter distance and larger acceleration gap, $T_2 < \hat{T}_2$, where $\hat{T}_2$ is the initially estimated time for Q_2. Since the satisfaction of initial feasibility suggests $\hat{T}_2 \leq Nt_{max}$, which leads to $T_2 \leq Nt_{max}$ that guarantees the feasibility of Q_2. Conversely, if $T_1 \leq Nt_{max}$, solution from $\mathbf{x}_e$ to $\mathbf{p}_1$ always exists. This completes the proof. ■

The feasibility of Q_1 suggests that the path and control sequence planned at the current position can complete the overtaking action without collision. Whereas the feasibility of Q_2 suggests that there exist path and control sequence such that the ego vehicle can return back to its original lane without collision. When the veh_f is non-accelerating, we can ensure that Q_1 is feasible, and the overtaking action can be completed; when the feasibility of Q_1 is challenged due to the acceleration of veh_f, we have Q_2 as our formal safety solution that can lead the ego vehicle back to its original lane safely.

Remark 5.3: The optimisation problem Q_2 in the proposed dual TO-CBF-MPC framework also serves as a fault-tolerant mechanism that further ensures the safety of the synthesised control strategy under non-cooperative environments. That is, under the extended possible accelerating behaviour of veh_f making Q_1 unsolvable, our framework can enable the ego vehicle to turn back to its original position in $\mathcal{L}_{\text{ego}}$ safely. Overall, Theorems 5.1 and 5.2 show that our integrated framework can provide formal guarantees for general on-road overtaking problems under the potential opposing traffic.

Remark 5.4: Note that, the assumption that veh_f is accelerating or decelerating but not interchangeably is essential for the correctness of our method. Without this assumption, in fact, no safe control law exists. For example, suppose that, when the ego vehicle is trying to overtake the front vehicle in the adjacent lane, the front vehicle takes aggressive actions by exactly imitating the behaviour of the ego vehicle. That is, it accelerates as the ego vehicle accelerates, and decelerates as the ego vehicle decelerates. Then in this case, the ego vehicle can neither overtake nor merge back to the safe region. However, this scenario is usually considered as 'non-rational' or even illegal in our daily life. Particularly, as pointed out by the well-known Responsibility-Sensitive Safety (RSS) model in autonomous driving (Shalev-Shwartz et al., 2017), one vehicle must obey the RSS rules in order to not be the 'cause' of an accident, and this scenario is essentially a violation of the RSS rules.

5.3. Incorporating semi-autonomous vehicles

In Section 5.2, we have established a formal safety guarantee for the proposed dual TO-CBF-MPC framework under the assumption that the opposing vehicle is also autonomous. In this subsection, we further discuss how the formal safety guarantee can be carried to the case when veh_o is semi-autonomous (non-cooperative) by conservative analysis.

Since the behaviours of human driver are usually irregular, we set the maximum acceleration and speed limit to the semi-autonomous veh_o to get the over-approximated prediction horizon $\{\mathbf{x}_o\}^N$ based on our real-time measurement of its states at every time step. Then the decision making process are generally depending on three key status: time taken to complete Q_1, Q_2; the final planned state of veh_e, $x_{eQ_i}^N$, $i \in \{1, 2\}$; and the final predicted state of veh_o, $x_{oQ_i}^N$, $i \in \{1, 2\}$; where $\{\times\}_{Q_i}^N, i \in \{1, 2\}$ represents the predicted sequence of N corresponding states (or controls) in the curly brackets by solving the TO-CBF-MPC problem of Q_i; $\times_{Q_i}^k$ denotes the k^{th} entry of the corresponding sequence.

As depicted in Figure 5, when $T_1 > T_2$, our primary concern is the safety of the final state during overtaking. As the time taken to merge back to $\mathbf{p}_2$ is shorter than that of overtaking to $\mathbf{p}_1$, we can always merge back, as long as overtaking is possible. When $T_1 \leq T_2$, we must consider whether a solution exists for Q_2 if overtaking becomes infeasible (potentially due to the approaching behaviour of veh_o). Since merging back is not time-critical, safety takes precedence in ensuring the feasibility of Q_2. Thus, when the feasibility of Q_2 is at risk, i.e. $x_{oQ_2}^N$ is approaching $\mathbf{p}_2$, we abandon the overtaking process and apply the control planned by Q_2. Note that, if the feasibility of Q_2 is at risk when veh_e has already cut into $\mathcal{L}_{\text{ego}}$ in front of veh_f, we will

Table 1. Conditions for overtaking.

Conditions					
$T_1 > T_2$	$x_{o_{Q_1}}^N > x_{e_{Q_1}}^N$	$x_{o_{Q_2}}^N > x_g^2$	$y_e \in \mathcal{L}_{\text{ego}}$	Overtake	Go Back
•	•			√	
°	•		•	√	
°	•		°		√
	•	•		√	
	°				√

•: satisfies, °: violates, *else*: not care.

proceed to complete the overtaking process. Under all cases, whenever the feasibility of Q_1 is being challenged, we merge back. Our decision maker is briefly summarised in Table 1.

In Table 1, the first column states the condition that whether the estimated time for TO-CBF-MPC problem Q_1 is greater than that of Q_2; the second column represents whether the predicted final position of veh_o will collide with the planned final position of veh_f; the third column checks whether the merging back operation will be safe when $T_1 \leq T_2$; and the fourth column checks if the ego vehicle is already in $\mathcal{L}_{\text{ego}}$ at the moment. The details of our framework is presented in Algorithm 1.

Remark 5.5: As the above section suggests, our framework can also be applied to the scenario when the opposing vehicle is semi-autonomous or human-driver-based. In this case, we use the conservative analysis by assuming the maximum acceleration rate and the speed limit of the veh_o in the prediction horizon and using the decision table to aid the decision-making process. Although this setting will increase the conservativeness under a semi-autonomous scenario, it provides formal guarantees of safety under the worst case.

Algorithm 1: Two-way Road Overtaking Framework

Input: $N, \mathbf{p}_1, \mathbf{p}_2$
Output: $T_1, T_2, \{\mathbf{u}_e\}_{Q_1}^N, \{\mathbf{u}_e\}_{Q_2}^N$

```
overtaking = True
veh_o = False
do
    get relative position of veh_f w.r.t. veh_e
    set virtual points p_1 and p_2 according to veh_f
    detect veh_o
    if veh_o == True then
        get measurements x_o
        Add VL-CBF constraint (25)
        compute T_1, {x_e}^N_{Q_1}, {u_e}^N_{Q_1} via Q_1
        compute T_2, {x_e}^N_{Q_2}, {u_e}^N_{Q_2} via Q_2
        if veh_o Semi-autonomous then
            Estimate worst case {x_o}^N_{Q_1}, {x_o}^N_{Q_2}
            overtaking ← decision from Table 1
            if overtaking == False then
                break
        else
            if Q_1 infeasible then
                break
    apply u^1_{e_{Q_1}} via Q_1
while Q_1 not converged and overtaking == True;
do
    apply u^1_{e_{Q_2}} via Q_2
while Q_2 not converged and overtaking == False;
```

6. Simulation results

Having illustrated the proposed two-way road overtaking framework in the previous sections, we now demonstrate our algorithm through simulations. Note that, the colour convention for vehicles in the simulations are inherited from Section 2.

6.1. Simulation setups

In our simulations, the dimension and physical parameters of all vehicles involved are adapted from the Toyota Camry, with a length of 4.885 m and width of 1.840 m. The lane width is scaled according to averaged global standard of 3.5 m. Horizon length of the predicted steps is $N = 50$, and the maximum time resolution $t_{max} = 0.2$ s. The sampling rate towards the veh_o is 50 Hz. The maximum acceleration rate is set as $a_l = 8\, m/s^2$, and the turning limit is defined as $\beta_- = -\arcsin 0.3$, $\beta_+ = \arcsin 0.3$. The goal position for Q_1 and Q_2 are established as $\mathbf{p}_1 = [x_e, x_f + \phi v_f(t)]$, $\mathbf{p}_2 = [x_e, x_f - \phi v_f(t)]$ respectively, with $\phi = 1.8$ s as in Section 5.1. Adopting these values, the controller for the framework takes the specific form of two optimisation problems presented in (24), as organised in Figure 4. The control input space is defined as $\mathcal{U} =$

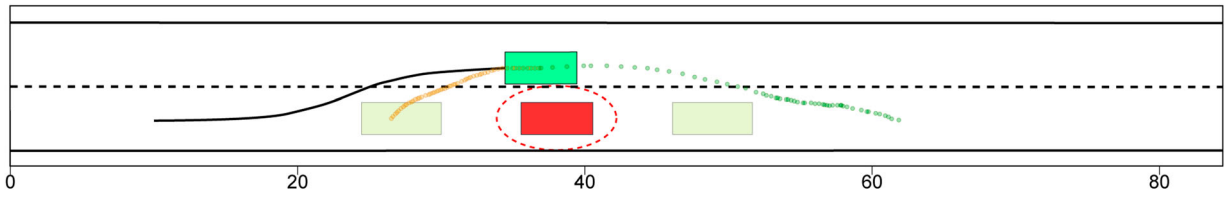

Figure 6. Overtaking with no opposing vehicle with constant velocity of the front vehicle at 8.3 m/s (30 km/h), and the velocity of the ego vehicle ranges from 10 to 19.4 m/s (36–70 km/h).

$([-a_l, a_l] \times [\beta_-, \beta_+])$, and the goal positions $\mathbf{p}_1$ and $\mathbf{p}_2$ are used for Q_1 and Q_2, respectively.

To further demonstrate the robustness of our method against uncertainties, random disturbances $\boldsymbol{\mu} = [\mu_x, \mu_y, \mu_v] \in \mathbb{R}^3$ are injected into the perception module, i.e. the state information used in the optimisation problem are the actual states with noises. Specifically, the perception noises are of uniform distribution such that: for the position information, we have $\mu_x, \mu_y \in [-0.5, 0.5]$ when the distance with the measured objects is greater than 2m, and $\mu_x, \mu_y \in [-0.1, 0.1]$ otherwise; and for velocity information, we have μ_v in the $\pm 10\%$ range of the actual velocity.

The TO-CBF-MPC optimisation problem in Equation (24) is implemented in `Python` with `CasADi` (Andersson et al., 2019) as modelling language, and is solved via IPOPT method (Biegler & Zavala, 2009) using a single performance core of the M1 Pro ARM processor.

6.2. Overtaking with no opposing vehicle

As illustrated in Figure 6, when there is no opposing traffic, the overall problem becomes a one-way road overtaking problem. During the overtaking process, the front vehicle veh_f can vary its speed, but it will adopt the rational driving behaviour as stated in Section 2. The reference goal positions $\mathbf{p}_1$ and $\mathbf{p}_2$ are displayed as the faded green rectangles in front of and behind the veh_f. The dashed ellipse around veh_f is the safety boundary enforced by the CBF based on the relative position between veh_e and veh_f.

In the simulation figures, the green and orange dotted circular trajectories represent the planned trajectory from $\mathbf{x}_e$ to $\mathbf{p}_1$ and $\mathbf{p}_2$ respectively derived through Q_1 and Q_2. The solid black line at the back of veh_e shows the actual trajectory travelled by the ego vehicle.

The time taken to overtake the front vehicle with different velocity configurations v_f are summarised in Table 2. For each group, 30 cases were simulated. The ego vehicle starts from the position at 10 m at 10 m/s (36 km/h), with an upper speed limit at 19.4 m/s (70 km/h). The front vehicle starts at 64 m. Note that, to cope with the introduced disturbances, the level set in the VL-CBF was set at $\epsilon = \tilde{\kappa}^{-1}(-\lambda_0) = 0.3$.

Table 2. Time taken when no opposing traffic.

Speed range of veh_e	36–70 km/h			
Speed of veh_f	25 km/h	28 km/h	32 km/h	36 km/h
min (s)	4.13	4.83	4.99	5.29
max (s)	5.27	5.94	6.44	6.63
mean (s)	4.64	5.02	5.59	5.90

6.3. Overtaking with opposing vehicles

For scenarios involving opposing vehicle during the overtaking process, we simulate various cases to demonstrate the effectiveness of our overall framework. All simulations are conducted with prediction horizon $N = 50$ and incorporate perception uncertainties as introduced in Section 6.1.

Case 1: veh_f is non-accelerating and veh_o is autonomous with a known VL-CBF strategy. In this scenario (Figure 7), a successful overtaking manoeuvre is demonstrated when both the ego vehicle (veh_f) and the opposing vehicle (veh_o) adhere to the VL-CBF safety control strategy. The dimmed and scattered dots represent planned trajectories with a prediction horizon of $N = 50$, while the black solid lines depict the actual trajectory of the ego vehicle. The simulation results demonstrate that, even in the presence of perception errors, the overtaking process remains not only safe but also closely aligns with the initially planned trajectories when both veh_f and veh_o adhere to the VL-CBF strategy.

Case 2: veh_f is non-accelerating and veh_o is human driver-based with an unknown strategy. In Figure 8, we illustrate a scenario where veh_o

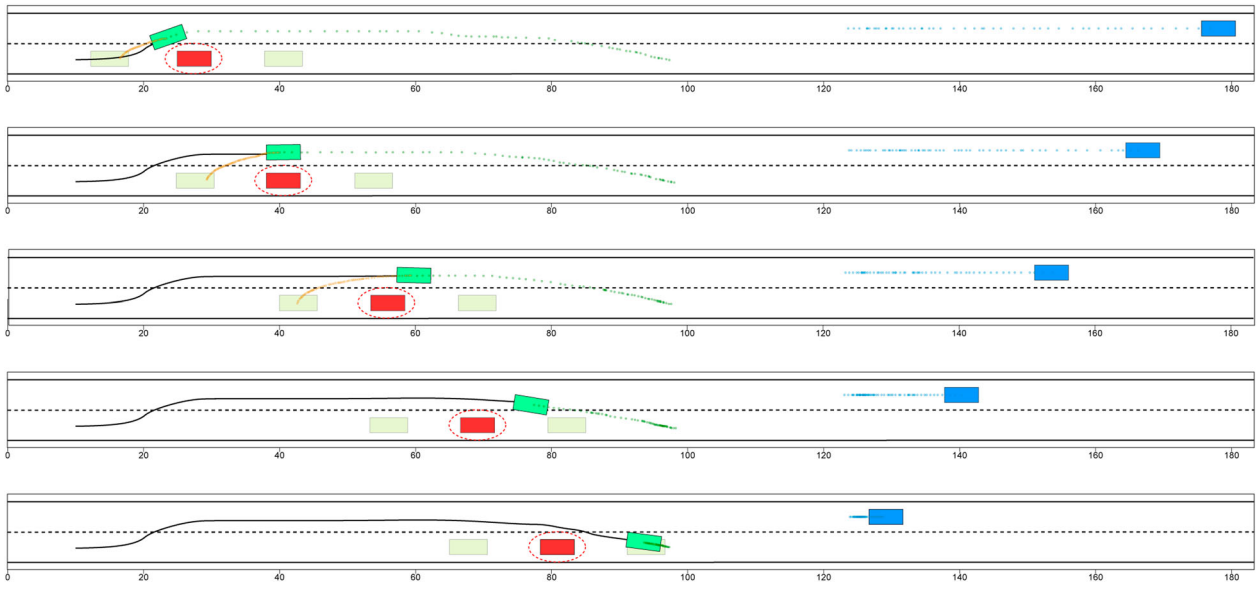

Figure 7. Snapshots from the simulation of the overtaking framework, with veh_f non-accelerating and veh_o fully autonomous.

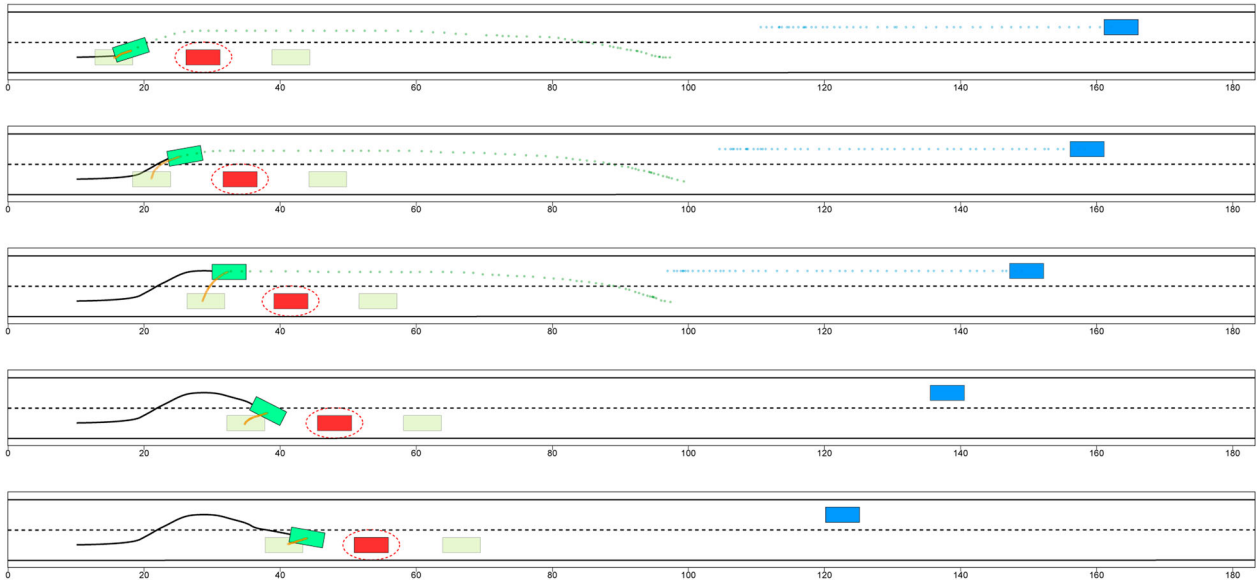

Figure 8. Snapshots from the simulation of the overtaking framework, with veh_f non-accelerating and veh_o human-driver-based and accelerating.

is human-driver-based, assumed to accelerate towards the speed limit at $\alpha_x^o = 1.6\,m/s$. In this case, the decision rules outlined in Table 1 for conservative analysis are active. The simulation shows that, when veh_o accelerates and the condition $x_{o_{Q_1}}^N \leq x_{e_{Q_1}}^N$ is activated, triggering the 'Goes Back' condition, the ego vehicle (veh_e) safely abandons the overtaking action.

Case 3: veh_f is accelerating and veh_o is autonomous with a known VL-CBF strategy. Even when the front vehicle (veh_f) is accelerating during the overtaking process, our method ensures safety by allowing the ego vehicle to return to its original position if overtaking becomes unsafe. We consider three different ranges of accelerating rates for veh_f, conducting 30 simulations for each range. Table 3 presents the minimum distance and the number of successful overtaking for each range. The results show that as the accelerating rate of veh_f increases, the chance of a successful overtaking task decreases. Nevertheless, the ego vehicle consistently maintains a safe distance outside the predefined ellipse-shaped safety region, even in cases where the overtaking task fails,

Table 3. Overtaking with different accelerating rates of veh_f.

	$\alpha_f^x \in (1,3]$	$\alpha_f^x \in (3,5]$	$\alpha_f^x \in (5,7]$
successful overtaking	29/30	11/30	0/30
min dist. with veh_f (m)	1.27	1.24	1.31
min dist. with veh_o (m)	18.31	5.52	72.41

which coincides with our objective of prioritising safety over task completion.

In summary, the simulation results presented in this subsection highlight the effectiveness of our proposed method across various driving scenarios. Our evaluation emphasises the safe-by-construction property of the framework, assuming rational behaviours of other vehicles (Shalev-Shwartz et al., 2017). This extends the applicability of our approach beyond existing safety-critical overtaking manoeuvres (He et al., 2021, 2022) to encompass general cases with potential opposing traffic on two-way road overtaking scenarios. The next section will provide a detailed comparison with the baseline approach.

6.4. Comparison with conventional MPC

In this subsection, we conduct simulations to further demonstrate the superiority of our approach. As discussed in Section 1.3.3, existing overtaking manoeuvres with safety guarantees cannot be directly extended to the case with opposing vehicles. Whereas if formal safety guarantee is not required, the conventional MPC-based method can be extended to the case with opposing vehicles by further considering the ellipse-shaped distance around the opposing vehicle as new distance constraints, known as MPC distances constraints (MPC-DC) (Zeng et al., 2021). Therefore, we compare the proposed dual TO-CBF-MPC approach with the standard MPC-DC for some extreme scenarios where the MPC-DC method may not be safe.

Specifically, we consider two simulation scenarios (A and B), where the velocities of veh_f and veh_o are constant during the simulation, i.e. veh_o is assumed to be unknown human driver with constant velocity. The velocities of veh_o are the same in two scenarios, but the velocity of veh_f in Scenario A is fast than that in Scenario B. Therefore, feasible overtaking actions in Scenario B may be dangerous in Scenario A.

For each scenario, the parameters for TO-CBF-MPC method and the MPC-DC method are as follows:

Table 4. Minimum distance with surrounding vehicles.

(Scenario A)	MPC-DC	$\epsilon = 0.3$	$\epsilon = 0.5$
min dist. with veh_f (m)	−0.15	0.76	0.99
min dist. with veh_o (m)	0.31	85.66	86.07
safe cases	0/30	30/30	30/30
(Scenario B)	MPC-DC	$\epsilon = 0.3$	$\epsilon = 0.5$
min dist. with veh_f (m)	0.37	0.77	1.02
min dist. with veh_o (m)	36.46	42.51	41.55
safe cases	19/30	30/30	30/30

(1) For the dual TO-CBF-MPC method, we consider the setting in Case 2 as above with $N = 50$, and investigate two different VL-CBF levels $\epsilon = \tilde{\kappa}^{-1}(-\lambda_0) = 0.3$ and $\epsilon = 0.5$ respectively;
(2) For the MPC-DC method, we also let the prediction horizon $N_{\text{MPC}} = 50$, and the distance constraints are set as the ellipse-shaped constraints as in VL-CBF.

We simulate each scenario of two different methods with perception errors by repeating the simulation 30 times. The perception noises are randomly generated using the simulation setups in Section 6.1.

To compare the two approaches, we show the minimum distances with other vehicles as well as the number of safe simulation cases among the 30 cases for each method (one MPC-DC controller and two VL-CBF controllers with different parameters) in Table 4. The simulation results show that, for VL-CBF controllers with different levels, our framework can always guarantee safety under disturbances for all simulations generated. Furthermore, for both parameters, the safety margins w.r.t. other vehicles are more significant, which means that our method is more robust than the MPC-DC method.

In Figure 9, we provide visualised simulation results for a Scenario A case (Figure 9(a)) and a Scenario B case (Figure 9(a)).

For scenario A in Figure 9(a), the high speed of the opposing vehicle makes overtaking unfeasible for both methods. Standard MPC-DC lacks a backup strategy, leading to a dangerous collision as the opposing vehicle serves as a moving obstacle, rendering the MPC-DC optimisation problem unsolvable. In contrast, our proposed dual TO-CBF-MPC framework can automatically switch to optimisation problem Q_2 (detailed in Section 5.2) and guide the ego vehicle safely back to $\mathcal{L}_{\text{ego}}$, terminating the overtaking process.

For Scenario B in Figure 9(b), there exists adequate space ahead of the vehicle for safe overtaking, and the

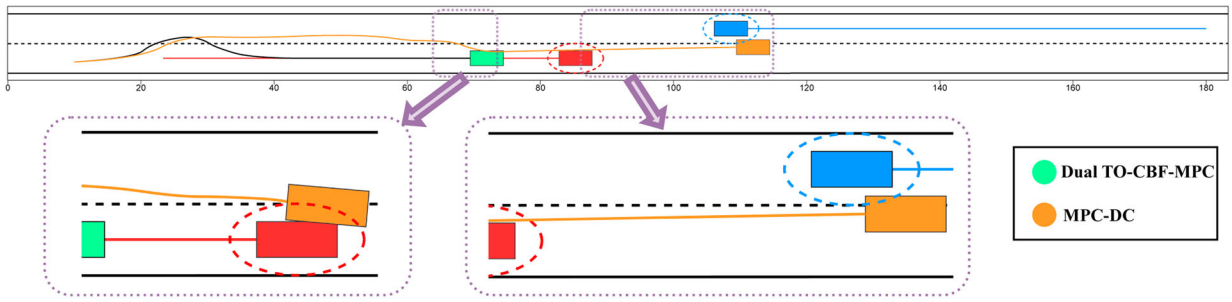

(a) Simulations for a Scenario A case, where our method will safely terminate the overtaking process when it is not feasible.

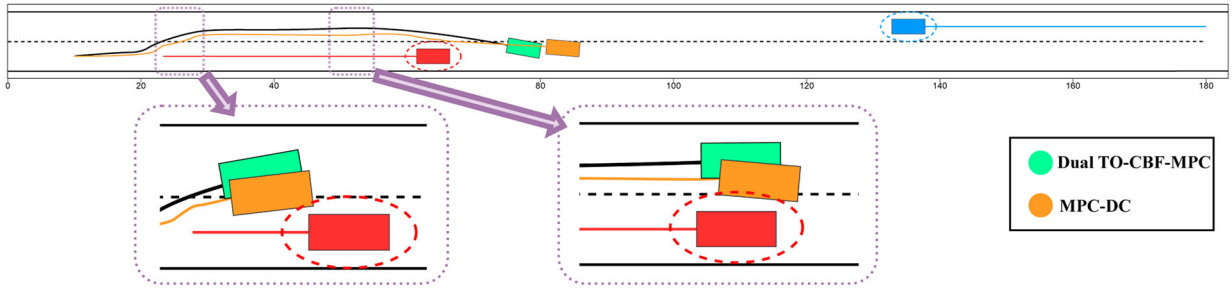

(b) Simulations for a Scenario B case, where our method can safely overtake the front vehicle but the existing method fails to do so.

Figure 9. Simulations of the proposed dual TO-CBF-MPC framework compared with the MPC-DC method with opposing traffic.

optimisation problem of MPC-DC method is always feasible. But safety is compromised due to violations of ellipse-shaped distance constraints caused by the inter-sampling effects and the introduced disturbances. Our proposed dual TO-CBF-MPC framework, on the other hand, plans trajectories with adjustable wider safety margins, ensuring safety even between sampling intervals and successfully mitigates the impact of disturbances. Specifically, as shown in Figure 9(b), the trajectory planned by the conventional MPC-DC method (depicted in orange) is significantly closer to the front vehicle than the trajectory planned by our proposed framework (depicted in black). At certain points, the orange trajectory even crosses the ellipse-shaped safety region, posing a potential threat to safety.

7. Conclusions

In this paper, we presented a novel safe-by-construction control framework for the general on-road overtaking scenarios with consideration of the potential opposing traffics. We showed the forward invariance of the property of an arbitrary user-defined super-level set enforced by the proposed VL-CBF and provided theoretical proof of the formal safety guarantees of our integrated framework. We demonstrated the effectiveness of combined framework via simulations of the proposed algorithm.

In the future, we plan to extend our framework to ensure probabilistic safety guarantees under imprecise system models, as well as exploiting methods like (Luo, Wang, Dong et al., 2023; Luo, Wang, Hu et al., 2023) to consider robust parameter tuning and security control under attacks. We also intend to explore the integration of an event-triggered control approach into our framework to further reduce computational burden by employing lower control frequencies, enhancing the energy efficiency of vehicle control.

Acknowledgments

The data that support the findings of this study are available from the corresponding author, D. Yuan, upon reasonable request.

Disclosure statement

No potential conflict of interest was reported by the author(s).

Funding

This work was supported by the National Key Research and Development Program of China (2018AAA0101700) and the National Natural Science Foundation of China (62061136004, 61803259, 61833012).

References

Agrawal, A., & Sreenath, K. (2017). Discrete control barrier functions for safety-critical control of discrete systems with application to bipedal robot navigation. In *Robotics: Science and systems XIII*. Robotics: Science and Systems Foundation.

Althoff, M., Maierhofer, S., & Pek, C. (2021, March). Provably-correct and comfortable adaptive cruise control. *IEEE Transactions on Intelligent Vehicles*, *6*(1), 159–174. https://doi.org/10.1109/TIV

Ames, A. D., Coogan, S., Egerstedt, M., Notomista, G., Sreenath, K., & Tabuada, P. (2019). Control barrier functions: Theory and applications. In *18th European control conference (ECC)* (pp. 3420–3431). IEEE.

Ames, A. D., Xu, X., Grizzle, J. W., & Tabuada, P. (2017). Control barrier function based quadratic programs for safety critical systems. *IEEE Transactions on Automatic Control*, *62*(8), 3861–3876. https://doi.org/10.1109/TAC.2016.2638961

Andersson, J. A. E., Gillis, J., Horn, G., Rawlings, J. B., & Diehl, M. (2019, March). CasADi: A software framework for nonlinear optimization and optimal control. *Mathematical Programming Computation*, *11*(1), 1–36. https://doi.org/10.1007/s12532-018-0139-4

Biegler, L. T., & Zavala, V. M. (2009, March). Large-scale nonlinear programming using IPOPT: An integrating framework for enterprise-wide dynamic optimization. *Computers & Chemical Engineering*, *33*(3), 575–582. https://doi.org/10.1016/j.compchemeng.2008.08.006

Blanchini, F. (1999, November). Set invariance in control. *Automatica*, *35*(11), 1747–1767. https://doi.org/10.1016/S0005-1098(99)00113-2

Chae, H., & Yi, K. (2020). Virtual target-based overtaking decision, motion planning, and control of autonomous vehicles. *IEEE Access*, *8*, 51363–51376. https://doi.org/10.1109/Access.6287639

Chen, J., Li, S. E., & Tomizuka, M. (2021). Interpretable end-to-end urban autonomous driving with latent deep reinforcement learning. *IEEE Transactions on Intelligent Transportation Systems*, *23*(6), 5068–5078. https://doi.org/10.1109/TITS.2020.3046646

Choi, J. J., Lee, D., Sreenath, K., Tomlin, C. J., & Herbert, S. L. (2021, December). Robust control barrier–value functions for safety-critical control. In *2021 60th IEEE conference on decision and control (CDC)* (pp. 6814–6821). IEEE.

Dawson, C., Lowenkamp, B., Goff, D., & Fan, C. (2022, April). Learning safe, generalizable perception-based hybrid control with certificates. *IEEE Robotics and Automation Letters*, *7*(2), 1904–1911. https://doi.org/10.1109/LRA.2022.3141657

Diaz Alonso, J., Ros Vidal, E., Rotter, A., & Muhlenberg, M. (2008, September). Lane-change decision aid system based on motion-driven vehicle tracking. *IEEE Transactions on Vehicular Technology*, *57*(5), 2736–2746. https://doi.org/10.1109/TVT.2008.917220

Dixit, S., Montanaro, U., Dianati, M., Oxtoby, D., Mizutani, T., Mouzakitis, A., & Fallah, S. (2019). Trajectory planning for autonomous high-speed overtaking in structured environments using robust MPC. *IEEE Transactions on Intelligent Transportation Systems*, *21*(6), 2310–2323. https://doi.org/10.1109/TITS.6979

Do, Q. H., Tehrani, H., Mita, S., Egawa, M., Muto, K., & Yoneda, K. (2017). Human drivers based active-passive model for automated lane change. *IEEE Intelligent Transportation Systems Magazine*, *9*(1), 42–56. https://doi.org/10.1109/MITS.2016.2613913

He, S., Zeng, J., & Sreenath, K. (2022, May). Autonomous racing with multiple vehicles using a parallelized optimization with safety guarantee using control barrier functions. In *2022 International conference on robotics and automation (ICRA)* (pp. 3444–3451). IEEE.

He, S., Zeng, J., Zhang, B., & Sreenath, K. (2021). Rule-based safety-critical control design using control barrier functions with application to autonomous lane change. In *2021 American control conference (ACC)* (pp. 178–185). IEEE.

Herbert, S., Choi, J. J., Sanjeev, S., Gibson, M., Sreenath, K., & Tomlin, C. J. (2021, May). Scalable learning of safety guarantees for autonomous systems using Hamilton-Jacobi reachability. In *IEEE international conference on robotics and automation (ICRA)* (pp. 5914–5920). IEEE.

Hu, J., Zhang, H., Liu, H., & Yu, X. (2021). A survey on sliding mode control for networked control systems. *International Journal of Systems Science*, *52*(6), 1129–1147. https://doi.org/10.1080/00207721.2021.1885082

Hu, X., Wu, L., Hu, C., Wang, Z., & Gao, H. (2014, August). Dynamic output feedback control of a flexible air-breathing hypersonic vehicle via T–S fuzzy approach. *International Journal of Systems Science*, *45*(8), 1740–1756. https://doi.org/10.1080/00207721.2012.749547

Khalil, H. K. (2015). *Nonlinear systems*. Pearson.

Kong, J., Pfeiffer, M., Schildbach, G., & Borrelli, F. (2015). Kinematic and dynamic vehicle models for autonomous driving control design. In *2015 IEEE intelligent vehicles symposium (IV)* (pp. 1094–1099). IEEE.

Li, X., Qiu, X., Wang, J., & Shen, Y. (2020, June). A deep reinforcement learning based approach for autonomous overtaking. In *2020 IEEE international conference on communications workshops (ICC Workshops)* (pp. 1–5). IEEE.

Li, X., Tan, J., Liu, A., Vijayakumar, P., Kumar, N., & Alazab, M. (2020). A novel UAV-enabled data collection scheme for intelligent transportation system through UAV speed control. *IEEE Transactions on Intelligent Transportation Systems*, *22*(4), 2100–2110. https://doi.org/10.1109/TITS.2020.3040557

Liang, X., Wang, T., Yang, L., & Xing, E. (2018). Cirl: Controllable imitative reinforcement learning for vision-based self-driving. In *Proceedings of the European conference on computer vision (ECCV)* (pp. 584–599). Springer.

Liu, X., Huang, C., Wang, Y., Zheng, B., & Zhu, Q. (2022, May). Physics-aware safety-assured design of hierarchical neural network based planner. In *2022 ACM/IEEE 13th international conference on cyber-physical systems (ICCPS)* (pp. 137–146). IEEE.

Liu, X., Jiao, R., Zheng, B., Liang, D., & Zhu, Q. (2023). Safety-driven interactive planning for neural network-based lane changing. In *Proceedings of the 28th Asia and South Pacific design automation conference* (pp. 39–45).

Luo, Y., Wang, Z., Chen, Y., & Yi, X. (2021, April). H_{infty} state estimation for coupled stochastic complex networks with periodical communication protocol and intermittent nonlinearity switching. *IEEE Transactions on Network Science and Engineering*, *8*(2), 1414–1425. https://doi.org/10.1109/TNSE.2021.3058220

Luo, Y., Wang, Z., Dong, H., Mao, J., & Alsaadi, F. E. (2023, July). A novel sequential switching quadratic particle swarm optimization scheme with applications to fast tuning of PID controllers. *Information Sciences*, *633*, 305–320. https://doi.org/10.1016/j.ins.2023.03.011

Luo, Y., Wang, Z., Hu, J., Dong, H., & Yue, D. (2023, October). Security-guaranteed fuzzy networked state estimation for 2-D systems with multiple sensor arrays subject to deception attacks. *IEEE Transactions on Fuzzy Systems*, *31*(10), 3624–3638. https://doi.org/10.1109/TFUZZ.2023.3262609

Luo, Y., Wang, Z., Sheng, W., & Yue, D. (2023, March). State estimation for discrete time-delayed impulsive neural networks under communication constraints: A delay-range-dependent approach. *IEEE Transactions on Neural Networks and Learning Systems*, *34*(3), 1489–1501. https://doi.org/10.1109/TNNLS.2021.3105449

Lyu, Y., Luo, W., & Dolan, J. M. (2021, May), Probabilistic safety-assured adaptive merging control for autonomous vehicles. In *2021 IEEE International conference on robotics and automation (ICRA)* (pp. 10764–10770). IEEE.

Lyu, Y., Luo, W., & Dolan, J. M. (2022, February). Adaptive safe merging control for heterogeneous autonomous vehicles using parametric control barrier functions. In *2022 IEEE intelligent vehicles symposium (IV)* (pp. 542–547). IEEE.

Meng, Q., Zhao, T., Qian, C., Sun, Z.-y., & Ge, P. (2018). Integrated stability control of AFS and DYC for electric vehicle based on non-smooth control. *International Journal of Systems Science*, *49*(7), 1518–1528. https://doi.org/10.1080/00207721.2018.1460410

Milanés, V., Llorca, D. F., Villagrá, J., Pérez, J., Fernández, C., Parra, I., González, C., & Sotelo, M. A. (2012, February). Intelligent automatic overtaking system using vision for vehicle detection. *Expert Systems with Applications*, *39*(3), 3362–3373. https://doi.org/10.1016/j.eswa.2011.09.024

Naranjo, J. E., Gonzalez, C., Garcia, R., & de Pedro, T. (2008, September). Lane-change fuzzy control in autonomous vehicles for the overtaking maneuver. *IEEE Transactions on Intelligent Transportation Systems*, *9*(3), 438–450. https://doi.org/10.1109/TITS.2008.922880

Ngai, D. C. K., & Yung, N. H. C. (2011, June). A multiple-goal reinforcement learning method for complex vehicle overtaking maneuvers. *IEEE Transactions on Intelligent Transportation Systems*, *12*(2), 509–522. https://doi.org/10.1109/TITS.2011.2106158

Nguyen, Q., & Sreenath, K. (2016, July). Exponential control barrier functions for enforcing high relative-degree safety-critical constraints. In *2016 American control conference (ACC)* (pp. 322–328). IEEE.

Petrov, P., & Nashashibi, F. (2014, August). Modeling and nonlinear adaptive control for autonomous vehicle overtaking. *IEEE Transactions on Intelligent Transportation Systems*, *15*(4), 1643–1656. https://doi.org/10.1109/TITS.2014.2303995

Qin, Z., Zhang, K., Chen, Y., Chen, J., & Fan, C. (2021). Learning safe multi-agent control with decentralized neural barrier certificates. arXiv preprint arXiv:2101.05436.

Richter, T., Ruhl, S., Ortlepp, J., & Bakaba, E. (2017). Causes, consequences and countermeasures of overtaking accidents on two-lane rural roads. *Transportation Research Procedia*, *25*, 1989–2001. https://doi.org/10.1016/j.trpro.2017.05.395

Rosolia, U., & Borrelli, F. (2020, November). Learning how to autonomously race a car: A predictive control approach. *IEEE Transactions on Control Systems Technology*, *28*(6), 2713–2719. https://doi.org/10.1109/TCST.87

Shalev-Shwartz, S., Shammah, S., & Shashua, A. (2017). On a formal model of safe and scalable self-driving cars. Preprint, arXiv:1708.06374.

Usman, G., & Kunwar, F. (2009). Autonomous vehicle overtaking- an online solution. In *2009 IEEE international conference on automation and logistics* (pp. 596–601). IEEE.

Wang, Y., Zhan, S., Wang, Z., Huang, C., Wang, Z., Yang, Z., & Zhu, Q. (2023, May). Joint differentiable optimization and verification for certified reinforcement learning. In *Proceedings of the ACM/IEEE 14th International conference on cyber-physical systems (with CPS-IoT Week 2023)* (pp. 132–141). Association for Computing Machinery.

Wang, Z., Ramyar, S., Salaken, S. M., Homaifar, A., Nahavandi, S., & Karimoddini, A. (2017, June). A collision avoidance system with fuzzy danger level detection. In *2017 IEEE intelligent vehicles symposium (IV)* (pp. 283–288). IEEE.

Xiao, W., & Belta, C. (2022). High-order control barrier functions. *IEEE Transactions on Automatic Control*, *67*(7), 3655–3662. https://doi.org/10.1109/TAC.2021.3105491

Xiao, W., Belta, C., & Cassandras, C. G. (2022a, May). Adaptive control barrier functions. *IEEE Transactions on Automatic Control*, *67*(5), 2267–2281. https://doi.org/10.1109/TAC.2021.3074895

Xiao, W., Belta, C. A., & Cassandras, C. G. (2022b, January). Sufficient conditions for feasibility of optimal control problems using control barrier functions. *Automatica*, *135*, 109960. https://doi.org/10.1016/j.automatica.2021.109960

Xiao, W., Wang, T.-H., Chahine, M., Amini, A., Hasani, R., & Rus, D. (2022c). Differentiable control barrier functions for vision-based end-to-end autonomous driving. arXiv preprint arXiv:2203.02401.

Xie, S., Hu, J., Bhowmick, P., Ding, Z., & Arvin, F. (2022, November). Distributed motion planning for safe autonomous vehicle overtaking via artificial potential field. *IEEE*

Transactions on Intelligent Transportation Systems, *23*(11), 21531–21547. https://doi.org/10.1109/TITS.2022.3189741

Xiong, Y., Zhai, D.-H., Tavakoli, M., & Xia, Y. (2022). Discrete-time control barrier function: High-order case and adaptive case. *IEEE Transactions on Cybernetics*, *53*(5), 1–9. https://doi.org/10.1109/TCYB.2022.3213597

Xu, K., Cassandras, C. G., & Xiao, W. (2022). Decentralized time and energy-optimal control of connected and automated vehicles in a roundabout with safety and comfort guarantees. *IEEE Transactions on Intelligent Transportation Systems*, *24*(1), 657–672. https://doi.org/10.1109/TITS.2022.3216794

Xu, X., Grizzle, J. W., Tabuada, P., & Ames, A. D. (2018, July). Correctness guarantees for the composition of lane keeping and adaptive cruise control. *IEEE Transactions on Automation Science and Engineering*, *15*(3), 1216–1229. https://doi.org/10.1109/TASE.2017.2760863

Yang, S., Chen, S., Preciado, V. M., & Mangharam, R. (2023). Differentiable safe controller design through control barrier functions. *IEEE Control Systems Letters*, *7*, 1207–1212. https://doi.org/10.1109/LCSYS.2022.3233322

Zeng, J., Zhang, B., & Sreenath, K. (2021, May). Safety-critical model predictive control with discrete-time control barrier function. In *2021 American control conference (ACC)* (pp. 3882–3889). IEEE.

Zhou, Z., Dong, X., Li, Z., Yu, K., Ding, C., & Yang, Y. (2022). Spatio-temporal feature encoding for traffic accident detection in VANET environment. *IEEE Transactions on Intelligent Transportation Systems*, *23*(10), 19772–19781. https://doi.org/10.1109/TITS.2022.3147826